

## Hydrogen-Assisted 1,2-Dichloroethane Dechlorination Catalyzed by Pt–Cu/SiO<sub>2</sub>: Evidence for Different Functions of Pt and Cu Sites

Victor Yu. Borovkov,<sup>†</sup> David R. Luebke, Vladimir I. Kovalchuk, and Julie L. d'Itri\*

Department of Chemical Engineering, University of Pittsburgh, Pittsburgh, Pennsylvania 15261

Received: January 10, 2003; In Final Form: April 8, 2003

A monometallic Pt/SiO<sub>2</sub> and two bimetallic Pt–Cu/SiO<sub>2</sub> with Pt/Cu atomic ratio of 1 (Pt1Cu1) and 0.33 (Pt1Cu3) have been investigated by a combination of reaction kinetics and FTIR spectroscopic studies in order to understand the factors that control the selectivity toward ethylene and ethane in the CH<sub>2</sub>Cl–CH<sub>2</sub>Cl + H<sub>2</sub> reaction. Carbon monoxide adsorption was used to probe the electronic state (ligand effect) of Pt and Cu, and the selective poisoning of Pt sites with CO under catalytic reaction conditions was employed to elucidate the impact of the ensemble effect and the role of Pt and Cu sites in the conversion of 1,2-dichloroethane. It was shown that both Pt and Cu in the bimetallic Pt–Cu catalysts are modified electronically, but this modification does not impact the catalysts' selectivity patterns. However, the addition of CO into the CH<sub>2</sub>Cl–CH<sub>2</sub>Cl + H<sub>2</sub> reaction mixture at 473 K to block Pt sites resulted in a significant improvement in the ethylene selectivity of the bimetallic catalysts at the expense of ethane. The observations are consistent with the idea that with the Pt–Cu catalysts, ethylene forms on Cu sites and the role of Pt is to produce a limited supply of dissociated H atoms that spill over to Cu and react thereon with adsorbed Cl atoms.

### Introduction

Previous research has shown that addition of Cu to Pt catalysts enhances the selectivity toward olefins in the reaction of vicinal alkyldichlorides with hydrogen and decreases the selectivity toward paraffins.<sup>1–4</sup> The ethylene selectivity of the Pt–Cu catalysts in the hydrogen-assisted dechlorination of 1,2-dichloroethane can approach 100% depending on the atomic ratio of Pt to Cu.<sup>1,3,4</sup> In addition, the selectivity is a strong function of time on stream. It is relatively low initially, approaching its steady-state value in several tens of hours.<sup>1,3</sup> The latter was explained by continuous alloying of the metallic components of the catalysts initially located apart because of chromatographic separation during catalyst preparation by impregnation of the support with inorganic salts of Pt and Cu.<sup>3</sup> However, direct experimental evidence for enhancing the degree of alloying of Pt and Cu in the course of the reaction was not provided.

There are many examples in which alloying results in significant changes in catalytic performance compared to that of the individual alloy components. In the case of Pt–Cu particles, Cu can donate electron density to the incompletely filled d-bands of Pt (ligand effect<sup>5</sup>). Copper may also decrease the average number of contiguous Pt atoms at the surface that participate in the reaction by simple dilution (ensemble effect<sup>6</sup>). In addition, alloying can influence the adsorption energies of reactants and reaction products thereby changing the catalyst activity,<sup>7</sup> or it can suppress side reactions resulting in a change in catalyst selectivity.<sup>8,9</sup>

One means of effectively probing both ligand and ensemble effects is the examination of CO adsorption on alloys using IR

spectroscopy. This technique has been used extensively, especially for the investigation of Pt-containing bimetallic alloy catalysts.<sup>2,10–13</sup> The value of the singleton frequency of CO adsorbed on Pt is a measure of the degree of electron density transfer to or from Pt, whereas the CO band frequency shift resulting from dipole–dipole coupling provides information about the size of Pt ensembles.<sup>14–18</sup> On the basis of the analysis of the dipole–dipole coupling frequency shifts, the singleton frequencies of CO adsorbed on Pt, and the chemical reaction kinetics, it was concluded that ligand effect does not affect the ethylene selectivity of Pt–Cu/SiO<sub>2</sub> catalysts in hydrogen-assisted dechlorination of 1,2-dichloroethane.<sup>2</sup> It was also suggested that ethylene forms on Cu sites and the role of Pt is to provide dissociated H atoms that spill over onto the Cu and react thereon with adsorbed Cl atoms to regenerate the catalytically active sites. However, no direct evidence to support this hypothesis was provided; also, no conclusion was made on the electronic state of Cu.

The objectives of the present investigation were to probe by FTIR study of CO adsorption the alloying and the electronic state of both Pt and Cu in bimetallic Pt–Cu/SiO<sub>2</sub> catalysts and to obtain experimental evidence for different function of Pt and Cu sites in the hydrogen-assisted dechlorination of 1,2-dichloroethane. For the latter, the Pt sites of Pt–Cu alloy particles were selectively blocked for 1,2-dichloroethane adsorption with CO.

### Experimental Section

The catalysts were prepared by pore volume impregnation of SiO<sub>2</sub> (Aldrich, 99+%, 60–100 mesh, 300 m<sup>2</sup> g<sup>−1</sup>, average pore diameter, 150 Å) with a 0.1 N aqueous HCl solution containing H<sub>2</sub>PtCl<sub>6</sub>·6H<sub>2</sub>O (Alfa, 99.9%) or a mixture of H<sub>2</sub>PtCl<sub>6</sub>·6H<sub>2</sub>O and CuCl<sub>2</sub>·2H<sub>2</sub>O (MCB Manufacturing Chemists, 99.5%), as described elsewhere.<sup>1</sup> The concentrations of the

\* Author to whom correspondence should be addressed. E-mail: jdtri@pitt.edu.

<sup>†</sup> Permanent address: N. D. Zelinsky Institute of Organic Chemistry, 117334 Moscow, Russia.

metals in the impregnating solutions were adjusted to obtain metal loadings of 2.4% for Pt/SiO<sub>2</sub>, and 3.0% Pt + 1.0% Cu and 3.0% Pt + 2.9% Cu for the two Pt–Cu/SiO<sub>2</sub>. The bimetallic catalysts had Pt/Cu atomic ratios of 1:1 (Pt1Cu1) and 1:3 (Pt1Cu3), respectively. The fraction of Pt atoms exposed after reduction at 493 K, as determined by CO chemisorption,<sup>1</sup> was 43, 10, and 4% for the Pt, Pt1Cu1, and Pt1Cu3, respectively. The average metal particle size for the catalysts, determined by TEM measurements using electron microscope JEM 2010 with a resolution of 0.14 nm and accelerating voltage of 200 kV as described elsewhere,<sup>19</sup> was 2.8, 3.4, and 3.2 nm for the Pt, Pt1Cu1, and Pt1Cu3 catalysts, respectively, reduced at 493 K.

The infrared spectra were recorded with a Research Series II FTIR spectrometer (Mattson, Inc.) equipped with a liquid N<sub>2</sub> cooled MCT detector. The IR cell was similar to that described elsewhere.<sup>20</sup> The cell volume was 200 cm<sup>3</sup> and the light path length was approximately 15 cm. The cell was equipped with glass stopcocks connected to gas inlet/outlet ports. The spectra of adsorbed CO were measured with a resolution of 2 or 4 cm<sup>-1</sup>, and 400 scans were accumulated per spectrum. The spectra of gaseous products of the reaction of 1,2-dichloroethane with H<sub>2</sub> were measured with a resolution of 2 cm<sup>-1</sup>, and 128 scans were accumulated per spectrum.

The infrared spectra were collected in the transmission mode, which mandates the use of thin wafers of the catalyst sample. The self-supporting catalyst wafers (~20 mg/cm<sup>2</sup> thick) were prepared by powdering the catalyst material in an agate mortar and then by pressing the powder at 830 atm for 3 min. Such catalyst wafers are hereinafter referred to as "fresh." The wafers were pretreated *in situ* by evacuating at 403 K for 1 h, then heating in flowing 5% H<sub>2</sub> + 95% He (both Praxair, 99.999+%) mixture (80 mL/min) to 493 K at 5 K/min and holding at this temperature for 1 h. Then, the gas phase was evacuated at 493 K to a pressure of 1 × 10<sup>-5</sup> Torr.

The dipole–dipole coupling frequency shifts and singleton frequencies of CO adsorbed on the catalyst were measured by means of a modified isotopic dilution method<sup>21</sup> using mixtures of <sup>13</sup>C<sup>18</sup>O (Isotec, 99+%, <sup>13</sup>C, 95+%, <sup>18</sup>O) and <sup>12</sup>C<sup>16</sup>O (Praxair, 99.99+%) of different compositions. Initially, the mixture of known composition was adsorbed on the pretreated sample at room temperature and an equilibrium pressure of 12 Torr. After 20 min the spectrum of adsorbed CO in the presence of gas phase was recorded, then the gaseous CO was evacuated at the same temperature for 20 min, and the spectrum of adsorbed CO was recorded in the absence of gas phase. By repeating the experiment while systematically changing the composition of the isotopic mixture, the spectra of adsorbed CO as a function of <sup>13</sup>C<sup>18</sup>O + <sup>12</sup>C<sup>16</sup>O mixture composition were determined. Because the number of gaseous CO molecules in the IR cell significantly exceeded the number of Pt atoms in the wafer, it was assumed that the composition of adsorbed layer was similar to that of gaseous <sup>13</sup>C<sup>18</sup>O + <sup>12</sup>C<sup>16</sup>O mixture added. Thus, the ratio of isotopes in the gas phase was used to approximate that on the catalyst surface. The singleton frequencies for linearly adsorbed <sup>12</sup>C<sup>16</sup>O and <sup>13</sup>C<sup>18</sup>O on Pt were the band position for the corresponding adsorbed CO at its minimal concentration in the <sup>12</sup>C<sup>16</sup>O + <sup>13</sup>C<sup>18</sup>O gaseous mixture. The dipole–dipole coupling shifts were the difference between the band position of adsorbed carbon monoxide after evacuation at maximal concentration of <sup>12</sup>C<sup>16</sup>O (or <sup>13</sup>C<sup>18</sup>O) in the <sup>12</sup>C<sup>16</sup>O + <sup>13</sup>C<sup>18</sup>O mixture and the corresponding singleton frequency.

The kinetics of 1,2-dichloroethane conversion in the presence of H<sub>2</sub> was studied in both static and continuous flow reactors. The static system was the IR cell described earlier and

experiments were conducted at a reaction temperature of 523 K. The reaction mixture consisted of 7–10 Torr of CH<sub>2</sub>Cl–CH<sub>2</sub>Cl (Sigma-Aldrich, 99.8%) and a 5-fold excess of H<sub>2</sub>. For experiments in which CO was used as a site blocker, approximately 2 Torr of CO (Praxair, 99.99%) was admitted to the initial reaction mixture. The CH<sub>2</sub>Cl–CH<sub>2</sub>Cl conversion and the composition of the reaction products were determined from the band intensities in IR spectra of gaseous CH<sub>2</sub>Cl–CH<sub>2</sub>Cl (1238 cm<sup>-1</sup>), C<sub>2</sub>H<sub>4</sub> (950 cm<sup>-1</sup>), and C<sub>2</sub>H<sub>6</sub> (2970 cm<sup>-1</sup>). As the cell contents were not mixed, it is possible that the kinetics measurements were influenced by the diffusion of the gases. Thus, these results were used only for a qualitative analysis, and a quantitative investigation was conducted using a differential flow reactor system.

The flow kinetics experiments were conducted in a stainless steel, differential, flow reaction system equipped with a quartz microreactor (10 mm i.d.) in which the catalyst was supported on a quartz frit. The pretreatment gases and gaseous reactants were metered using mass flow controllers (Brooks, model 5850E) and mixed prior to entering the reactor. The 1,2-dichloroethane was metered into the system by flowing He through a saturator containing the liquid reactant. A constant inlet concentration was ensured by maintaining the saturator at a fixed temperature of 273 ± 1 K using a recirculating cooling system. The catalyst temperature was maintained ±1 K using an electric furnace and a temperature controller (Omega model CN2011). The reaction products were monitored online using a gas chromatograph (Varian 3300 series) equipped with a 10 ft 60/80 Carboxen B/5% Fluorocel packed column (Supelco) and a flame ionization detector. The detection limit for all products was 2 ppm. Hydrogen chloride was not quantified in these experiments.

The catalyst pretreatment consisted of flowing He (30 mL/min) for 5 min at 303 K. The He flow was continued as the catalyst was heated to 403 K at a rate of 6.7 K/min and held at 403 K for 1 h. Then, the flow was switched to 20% H<sub>2</sub> + 80% He (50 mL/min) and the catalyst was heated to 493 K at a rate of 6.7 K/min and held at 493 K for 1.5 h. The catalyst was then cooled in He (40 mL/min) to the reaction temperature.

The reaction was conducted at 473 K and atmospheric pressure. The total flow rate of the reaction mixture was 41 mL/min and consisted of 7000 ppm CH<sub>2</sub>ClCH<sub>2</sub>Cl, 36,600 ppm H<sub>2</sub>, and a balance of He. For some experiments, 1450 ppm of He was replaced with an equal volume of CO. The conversion was maintained in the differential range between 3 and 4%. Approximately 200 mg of catalyst were necessary to achieve this conversion, given the described flow rates and reaction temperature.

## Results

**Non-Steady-State Kinetics.** With a 5-fold excess of hydrogen, 1,2-dichloroethane was converted exclusively to ethane and HCl with both the Pt and the Pt1Cu1 catalysts (Figure 1). For the Pt1Cu3 catalysts, the reaction products were not only ethane and HCl but also ethylene (Figure 2). The initial selectivity of the Pt1Cu3 catalyst toward the formation of ethylene was 80%, but it gradually decreased to 65% during the 40 min reaction.

The addition of ~2 Torr of CO to the reaction mixture (50 Torr of H<sub>2</sub> + 10 Torr of CH<sub>2</sub>Cl–CH<sub>2</sub>Cl for the Pt, and 35 Torr of H<sub>2</sub> + 7 Torr of CH<sub>2</sub>Cl–CH<sub>2</sub>Cl for the Pt1Cu1) decreased the activity of the Pt and Pt1Cu1 catalysts by ~50 and 20%, respectively, in comparison to the results obtained when no CO was added. However, ethane was still the only carbon-containing product observed for both catalysts. The addition of CO

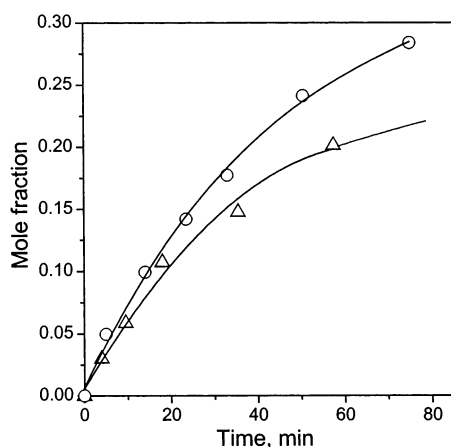


**Figure 1.** Dynamics of ethane accumulation in the catalyzed  $\text{CH}_2\text{ClCH}_2\text{Cl} + \text{H}_2$  reaction at 523 K in a static reactor; ( $\Delta$ ) Pt/SiO<sub>2</sub>, initial pressures of  $\text{CH}_2\text{ClCH}_2\text{Cl}$  and  $\text{H}_2$  were 10.0 and 50.0 Torr, respectively; (O) Pt1Cu1/SiO<sub>2</sub>, initial pressures of  $\text{CH}_2\text{ClCH}_2\text{Cl}$  and  $\text{H}_2$  were 7.0 and 35.0 Torr, respectively.

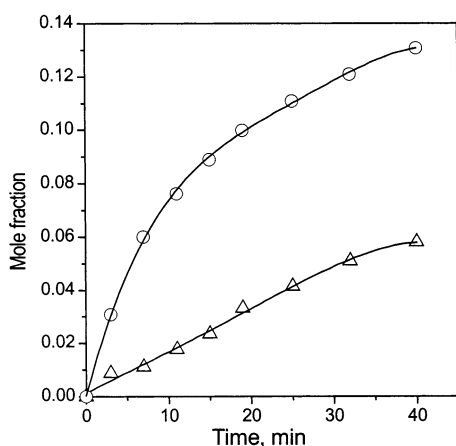


**Figure 2.** Dynamics of reaction product accumulation in the  $\text{CH}_2\text{ClCH}_2\text{Cl} + \text{H}_2$  reaction catalyzed by Pt1Cu3/SiO<sub>2</sub> at 523 K in a static reactor to form  $\text{C}_2\text{H}_4$  (O) and  $\text{C}_2\text{H}_6$  ( $\Delta$ ). Initial pressures of  $\text{CH}_2\text{ClCH}_2\text{Cl}$  and  $\text{H}_2$  were 7.8 and 50.0 Torr, respectively.

increased the selectivity of Pt1Cu3 catalyst toward ethylene from ~80 to 100% and this selectivity was independent of the 1,2-dichloroethane conversion (not shown). With respect to the activity of the Pt1Cu3 catalyst, the rate of conversion with and without CO was approximately the same (Figure 3).

After the Pt1Cu1 catalyst that was used in the  $\text{CH}_2\text{ClCH}_2\text{Cl} + \text{H}_2$  reaction shown in Figure 1 was heated in 35 Torr of CO at the temperature of 473 K for 0.5 h, its selectivity behavior in the presence of CO was significantly different than that of the fresh catalyst. The initial selectivity toward ethylene when 2 Torr of CO was present was ~100% (Figure 4). After 20 min, the concentration of ethylene reached a maximum of 5 mol % and remained constant thereafter. The selectivity toward ethane increased gradually from ~0% at zero contact time to 70% after 55 min.

It is worth mentioning that the influence of CO on the activity and selectivity of all the catalysts was reversible. Removing CO from the reactant mixture resulted in the same kinetics performance as that observed for catalysts that were not exposed to CO.

**Differential Flow Kinetics.** There was a substantial difference in the differential kinetics results obtained for the Pt1Cu1 catalyst when CO was added to the reactant stream and when it was not (Figure 5). Without CO in the reactant stream, ethane

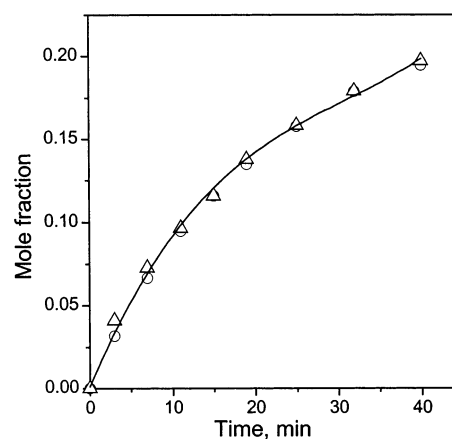


**Figure 3.** Dynamics of reaction product accumulation (a sum of ethane and ethylene) in the  $\text{CH}_2\text{ClCH}_2\text{Cl} + \text{H}_2$  reaction catalyzed by Pt1Cu3/SiO<sub>2</sub> at 523 K in a static reactor without ( $\Delta$ ) and with addition of 1.5 Torr CO (O). Initial pressures of  $\text{CH}_2\text{ClCH}_2\text{Cl}$  and  $\text{H}_2$  were 7.8 and 50.0 Torr, respectively.

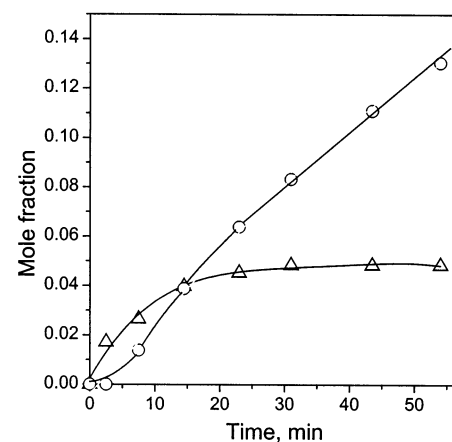


**Figure 4.** Dynamics of reaction product accumulation,  $\text{C}_2\text{H}_4$  ( $\Delta$ ) and  $\text{C}_2\text{H}_6$  (O), in the  $\text{CH}_2\text{ClCH}_2\text{Cl} + \text{H}_2$  reaction with CO addition in a static reactor at 523 K catalyzed by Pt1Cu1/SiO<sub>2</sub> sample that was used in the experiment shown in Figure 1 followed by heating in 35 Torr of CO at 473 K for 0.5 h. Initial pressures of  $\text{CH}_2\text{ClCH}_2\text{Cl}$ ,  $\text{H}_2$ , and CO were 9.0, 45.0, and 1.5 Torr, respectively.

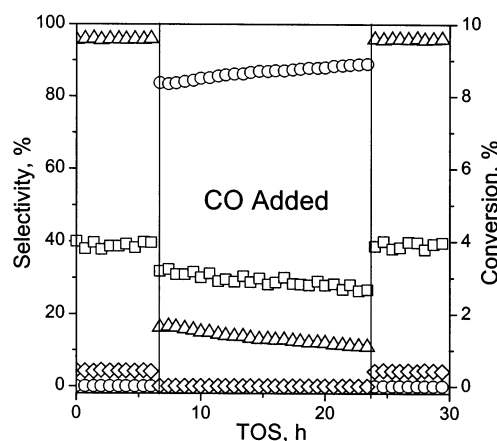


**Figure 5.** Time-on-stream performance of the Pt1Cu1/SiO<sub>2</sub> in the  $\text{CH}_2\text{ClCH}_2\text{Cl} + \text{H}_2$  reaction at 473 K in a continuous flow reactor with and without CO in the stream; (O), ethylene, ( $\Delta$ ), ethane, ( $\diamond$ ), ethyl chloride, ( $\square$ ), conversion.

was the main product with selectivity in excess of 95%; monochloroethane (5%) was also observed. When 1450 ppm of CO was added into the reaction mixture, ethylene was the

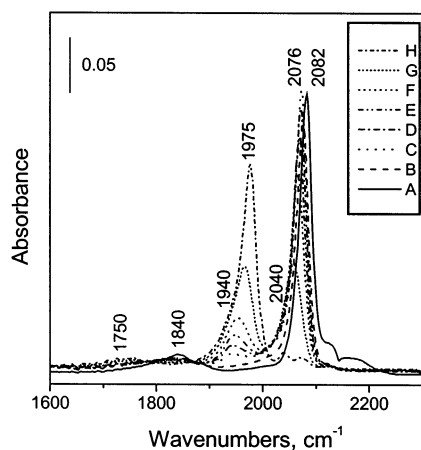


**Figure 6.** Dynamics of the exchange of  $^{12}\text{C}^{16}\text{O}$  pre-adsorbed on the reduced Pt/SiO<sub>2</sub> with gaseous  $^{13}\text{C}^{18}\text{O}$  at ambient temperature. (A) Spectrum of adsorbed  $^{12}\text{C}^{16}\text{O}$  in the presence of gas phase; (B) spectrum after evacuation at room temperature; (C)–(H) the spectra of adsorbed CO with the degree of  $^{12}\text{C}^{16}\text{O}$  exchange varying from 10 (C) to  $\sim 100\%$  (H).

main product ( $\sim 90\%$ ) and ethane was the minor product. When the CO was eliminated from the reactant stream, the initial selectivity was restored. The activity, which decreased by 25% upon addition of CO, also returned to its original level. The carbon monoxide was not consumed in the reaction.

**Spectral Measurements.** With 10 Torr of  $^{12}\text{C}^{16}\text{O}$  in the gas phase, the spectrum of  $^{12}\text{C}^{16}\text{O}$  adsorbed on a reduced fresh Pt catalyst consisted of an intense absorption band at  $2082\text{ cm}^{-1}$  and a weak band at  $1840\text{ cm}^{-1}$  (Figure 6), corresponding to linear and bridged modes, respectively.<sup>22,23</sup> The evacuation of the gas phase at room temperature resulted in a shift of the band assigned to linearly bonded  $^{12}\text{C}^{16}\text{O}$  from  $2082$  to  $2075\text{ cm}^{-1}$  as expected when the CO surface coverage decreases.<sup>24</sup> The admission of  $^{13}\text{C}^{18}\text{O} + ^{12}\text{C}^{16}\text{O}$  to the Pt catalyst pre-exposed to  $^{12}\text{C}^{16}\text{O}$  resulted in the partial replacement of adsorbed  $^{12}\text{C}^{16}\text{O}$  molecules by gaseous  $^{13}\text{C}^{18}\text{O}$  (Figure 6). As the exchange of adsorbed  $^{12}\text{C}^{16}\text{O}$  for  $^{13}\text{C}^{18}\text{O}$  progressed, the intensities of the bands corresponding to the linear and bridging forms of adsorbed  $^{12}\text{C}^{16}\text{O}$  decreased and the band attributed to linearly adsorbed  $^{12}\text{C}^{16}\text{O}$  shifted from  $2075$  to  $2040\text{ cm}^{-1}$ . This shift results from a weakening of dipole–dipole coupling between adsorbed  $^{12}\text{C}^{16}\text{O}$  molecules as the coverage decreased by substitution with the heavier isotopic  $^{13}\text{C}^{18}\text{O}$  molecules.<sup>18,21</sup> Simultaneously, the vibrational bands attributed to  $^{13}\text{C}^{18}\text{O}$  adsorbed on metallic Pt in linear and bridged forms appeared and increased in intensity. The bridging form of adsorbed  $^{13}\text{C}^{18}\text{O}$  is characterized by a low intensity band at  $1750\text{ cm}^{-1}$ . The band attributed to  $^{13}\text{C}^{18}\text{O}$  linearly adsorbed at a low degree of exchange of  $^{12}\text{C}^{16}\text{O}$  for  $^{13}\text{C}^{18}\text{O}$  appeared at  $1940\text{ cm}^{-1}$  and shifted to  $1975\text{ cm}^{-1}$  as the degree of exchange increased. Thus, the singleton frequencies for linearly adsorbed  $^{12}\text{C}^{16}\text{O}$  and  $^{13}\text{C}^{18}\text{O}$  on Pt were determined to be  $2040$  and  $1940\text{ cm}^{-1}$ , respectively. The dipole–dipole shifts for both isotopes were the same,  $35\text{ cm}^{-1}$ .

When the exchange experiment was conducted with the reduced PtCu1 catalyst, very different adsorption behavior was observed than that for Pt sample (Figure 7). At a  $^{12}\text{C}^{16}\text{O}$  equilibrium pressure of 10 Torr, the spectrum of adsorbed  $^{12}\text{C}^{16}\text{O}$  consisted of two absorption bands with maxima at  $2073$  and  $2135\text{ cm}^{-1}$ . These bands have been previously assigned to  $^{12}\text{C}^{16}\text{O}$  adsorbed linearly on metallic Pt ( $2073\text{ cm}^{-1}$ ) and Cu ( $2133\text{ cm}^{-1}$ ).<sup>18,24</sup> Evacuation of the  $^{12}\text{C}^{16}\text{O}$  at room temperature for 15 min resulted in the disappearance of the high-frequency

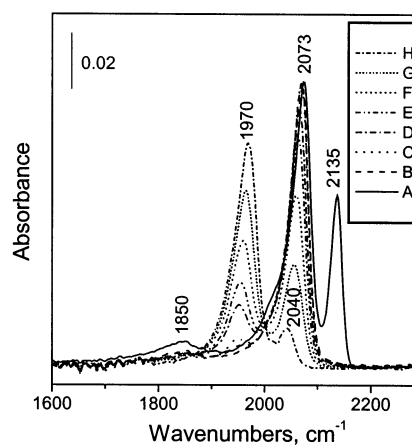


**Figure 7.** Dynamics of the exchange of  $^{12}\text{C}^{16}\text{O}$  pre-adsorbed on the reduced fresh PtCu1/SiO<sub>2</sub> with gaseous  $^{13}\text{C}^{18}\text{O}$  at ambient temperature. (A) Spectrum of adsorbed  $^{12}\text{C}^{16}\text{O}$  in the presence of gas phase; (B) the spectrum after evacuation at room temperature; (C)–(H) the spectra of adsorbed CO with the degree of  $^{12}\text{C}^{16}\text{O}$  exchange varying from 10 (C) to  $\sim 100\%$  (H).

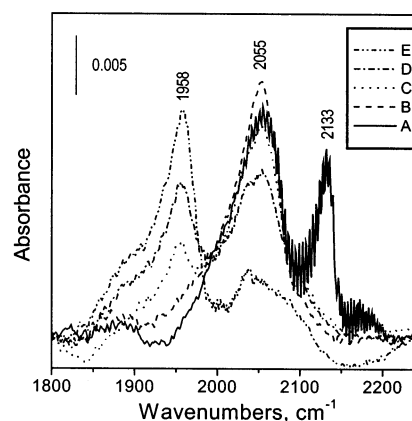


**Figure 8.** Dynamics of the exchange of  $^{12}\text{C}^{16}\text{O}$  pre-adsorbed on the PtCu1/SiO<sub>2</sub> that was used in the experiments depicted in the Figure 1 followed by heating the wafer in 35 Torr CO for 0.5 h at 473 K. (A) Spectrum of adsorbed  $^{12}\text{C}^{16}\text{O}$  in the presence of gas phase; (B) that after evacuation at room temperature; (C), (D), and (E) the spectra of adsorbed CO with the degree of  $^{12}\text{C}^{16}\text{O}$  exchange of 25, 40, and 65%, respectively.

band at  $2135\text{ cm}^{-1}$  and the shift of the  $2073\text{ cm}^{-1}$  band to  $2065\text{ cm}^{-1}$ . The disappearance of the band at  $2135\text{ cm}^{-1}$  upon room-temperature evacuation highlights thermal instability of the complexes of CO with Cu. During the exchange of pre-adsorbed  $^{12}\text{C}^{16}\text{O}$  for  $^{13}\text{C}^{18}\text{O}$ , the band of  $^{12}\text{C}^{16}\text{O}$  linearly adsorbed on Pt decreased in intensity and shifted from  $2065$  to  $2040\text{ cm}^{-1}$ . At a low degree of exchange, the band of linearly adsorbed  $^{13}\text{C}^{18}\text{O}$  on Pt appeared at  $1945\text{ cm}^{-1}$  and with increasing degree of exchange shifted to  $1970\text{ cm}^{-1}$ . Thus, similar to those for the monometallic Pt catalyst, the singleton frequencies for linearly adsorbed  $^{12}\text{C}^{16}\text{O}$  and  $^{13}\text{C}^{18}\text{O}$  on Pt of the PtCu1 catalyst were  $2040$  and  $1945\text{ cm}^{-1}$ , respectively; however, the dipole–dipole shift for both molecules was  $25\text{ cm}^{-1}$ .

After the reaction of  $\text{CH}_2\text{Cl}-\text{CH}_2\text{Cl}$  with  $\text{H}_2$  was performed on the PtCu1 catalyst wafer (Figure 1), it was heated in 35 Torr of CO at 473 K for 0.5 h. Figure 8 shows the spectrum evolution of  $^{12}\text{C}^{16}\text{O}$  and  $^{13}\text{C}^{18}\text{O}$  adsorbed on this catalyst during the exchange of pre-adsorbed  $^{12}\text{C}^{16}\text{O}$  for  $^{13}\text{C}^{18}\text{O}$ . In the presence of gaseous  $^{12}\text{C}^{16}\text{O}$ , the spectrum consisted of two bands at  $2055$  and  $2135\text{ cm}^{-1}$ . These bands are attributed to  $^{12}\text{C}^{16}\text{O}$  molecules linearly adsorbed on metallic Pt and Cu, respectively. As in the case of the reduced fresh PtCu1 catalyst, the high-frequency



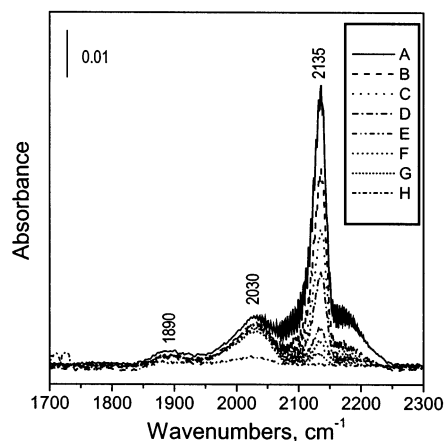


**Figure 9.** IR spectra of  $^{12}\text{C}^{16}\text{O}$  adsorbed on reduced  $\text{Pt1Cu3/SiO}_2$  at equilibrium pressures of 4.3 (A), 2.15 (B), 1.07 (C), 0.53 (D), 0.26 (E), 0.13 (F), 0.07 (G) Torr, and after evacuation of the sample with pre-adsorbed CO at room temperature for 12 h (H). Rotational structure seen in the spectra is a contribution from gas-phase CO.

band at  $2135\text{ cm}^{-1}$  disappeared after the sample was evacuated at room temperature for 15 min. During the exchange of pre-adsorbed  $^{12}\text{C}^{16}\text{O}$  for  $^{13}\text{C}^{18}\text{O}$ , the band maximum positions of both linearly adsorbed  $^{12}\text{C}^{16}\text{O}$  and  $^{13}\text{C}^{18}\text{O}$  remained essentially unchanged.

The spectra of  $^{12}\text{C}^{16}\text{O}$  adsorbed at different equilibrium pressures on the reduced fresh  $\text{Pt1Cu3}$  catalyst are shown in Figure 9. The band at  $2030\text{ cm}^{-1}$  has been assigned to linearly adsorbed CO on Pt, and the band at  $2135\text{ cm}^{-1}$  has been assigned to CO adsorbed on Cu.<sup>18,24</sup> A sharp decrease in intensity of the  $2135\text{ cm}^{-1}$  band occurred when the CO equilibrium pressure was decreased, demonstrating that the CO–Cu species are unstable. Decreasing the CO equilibrium pressure did not affect the positions of the band maxima for CO adsorbed on both Pt and Cu. However, after evacuation of the sample with pre-adsorbed CO for 12 h at room temperature, the  $2030\text{ cm}^{-1}$  band intensity decreased sharply and its maximum shifted  $2025\text{ cm}^{-1}$  (spectrum H in the Figure 9). Nevertheless, it is more consistent to consider  $2030\text{ cm}^{-1}$  as the singleton frequency for linearly adsorbed CO on Pt of the  $\text{Pt1Cu3}$  catalyst because, unlike the other singleton frequency measurements, the value of  $2025\text{ cm}^{-1}$  was obtained for CO coverage approaching zero, which is characteristic of the thermal desorption method,<sup>25</sup> different than that of the isotopic dilution. It is worth noting that the position of the  $^{12}\text{CO}$  band on Pt when mixtures of  $^{12}\text{CO}$  and  $^{13}\text{CO}$  of different compositions were adsorbed on a low metal loading Pt–Cu catalyst with the Pt/Cu atomic ratio of 0.3 was independent of the  $^{12}\text{CO}$  concentration in the  $^{12}\text{CO} + ^{13}\text{CO}$  mixture and the band was also located at  $2030\text{ cm}^{-1}$ .<sup>2</sup>

The spectra of CO adsorbed on  $\text{Pt1Cu3}$  in the presence of 6.7 Torr of CO (spectrum A) and of the mixture 6.7 Torr CO + 6.7 Torr  $\text{CH}_2\text{Cl}-\text{CH}_2\text{Cl}$  (spectrum B) are shown in Figure 10. Each spectrum consisted of two bands with maxima at 2030 and  $2136\text{ cm}^{-1}$  corresponding to CO linearly adsorbed on Pt and Cu, respectively. The presence of  $\text{CH}_2\text{Cl}-\text{CH}_2\text{Cl}$  in the IR cell did not affect the CO absorption band associated with Pt. However, the addition of  $\text{CH}_2\text{Cl}-\text{CH}_2\text{Cl}$  resulted in the decrease of the  $2136\text{ cm}^{-1}$  band intensity.

## Discussion

There are two reaction pathways for the conversion of vicinal alkyldichlorides by bimetallic Pt- and Pd-containing catalysts

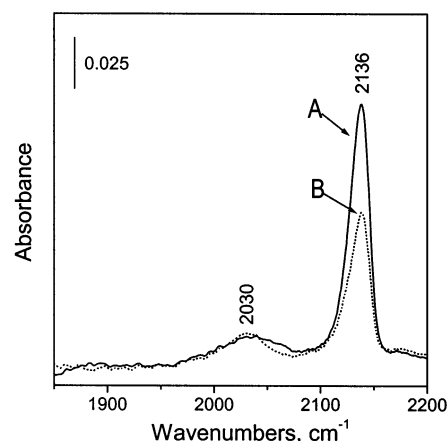


**Figure 10.** IR spectra of CO adsorbed on catalyst  $\text{Pt1Cu3/SiO}_2$  in the presence in the gas phase of 6.7 Torr CO (A) and of the mixture 6.7 Torr CO + 6.7 Torr  $\text{CH}_2\text{Cl}-\text{CH}_2\text{Cl}$  (B)

in the presence of  $\text{H}_2$ .<sup>1–4,26–28</sup> The first one, hydrodechlorination, results in the formation of alkanes, whereas the second, hydrogen-assisted dechlorination, leads to olefins. With 1,2-dichloroethane, the primary reaction intermediate is most likely the di- $\sigma$  complex of ethylene that forms via the homolytic dissociation of both C–Cl bonds of  $\text{CH}_2\text{Cl}-\text{CH}_2\text{Cl}$ .<sup>1,26</sup> This intermediate can either desorb into the gas phase as ethylene (hydrogen-assisted dechlorination pathway) or react with adsorbed H atoms to form ethane (hydrodechlorination pathway).

With little or no Cu in the catalyst, the hydrodechlorination chemistry dominates. At 523 K in the presence of excess of hydrogen, both monometallic Pt- and bimetallic  $\text{Pt1Cu1}$  exclusively converted  $\text{CH}_2\text{Cl}-\text{CH}_2\text{Cl}$  into HCl and ethane (Figure 1). The metallic Pt is responsible for the formation of this hydrocarbon.<sup>1–3,28</sup> Not surprisingly, the electronic state of Pt in the  $\text{Pt1Cu1}$  is similar to the monometallic Pt-sample, viz., the singleton frequencies ( $2040\text{ cm}^{-1}$ ) of the IR band of linearly adsorbed  $^{12}\text{C}^{16}\text{O}$  on metallic Pt were the same for both catalysts (Figures 6, 7).

One may question whether the Pt and Cu are alloyed in the reduced fresh  $\text{Pt1Cu1}$  catalyst, because of the similarities in the results for CO adsorption on Pt and the catalytic performance. However, the different effect of CO in the reaction mixture on the activity of the Pt and  $\text{Pt1Cu1}$  catalysts in the  $\text{CH}_2\text{Cl}-\text{CH}_2\text{Cl} + \text{H}_2$  reaction suggests that Pt and Cu interact in the  $\text{Pt1Cu1}$ . The formation of bimetallic Pt–Cu particles (probably, with the surface highly enriched in Pt) is also evident from the analyses of the spectra of CO adsorbed on Cu. There is a single absorption band with a maximum at  $2135\text{ cm}^{-1}$ , independent of CO surface coverage (Figure 7). The maximum frequency is  $40\text{ cm}^{-1}$  higher than that for CO linearly adsorbed on metallic Cu supported on alumina<sup>18</sup> or silica.<sup>24</sup> This peak cannot be assigned to complexes of CO with  $\text{Cu}^+$  ions because those species are stable in a vacuum at room temperature. Moreover, after reduction of the  $\text{Pt1Cu1}$  catalyst in hydrogen at temperature as high as 773 K, conditions at which  $\text{Cu}^+$  is definitely reduced,<sup>29</sup> the spectrum of CO adsorbed on Cu is also represented by a single band at  $\sim 2135\text{ cm}^{-1}$  (not shown). Thus, this band is attributed to complexes of CO with metallic Cu modified by Pt.<sup>18,24,29</sup>

The Pt in the  $\text{Pt1Cu3}$  catalyst has a different electronic signature than monometallic Pt or the Pt in the  $\text{Pt1Cu1}$ . The  $\text{Pt1Cu3}$  is characterized by a low singleton frequency of  $2030\text{ cm}^{-1}$  and the absence of dipole–dipole shift for linearly adsorbed CO (Figure 9). Such Pt modifications result most likely from the alloying of Pt and Cu such that the surface Pt atoms

are strongly diluted by atoms of Cu. Chandler and Pignolet studied CO adsorbed on a cluster-derived, silica-supported Pt–Cu catalyst with DRIFTS.<sup>30</sup> They attributed the small CO dipole–dipole interaction, with respect to that observed by others for coimpregnated catalysts, to more complete alloying in their bimetallic cluster-derived sample. Similarly, Grunert and co-workers interpreted the smaller CO dipole–dipole interactions obtained with ZSM-5 supported Pt–Cu catalysts after repeated oxidation and reduction cycles in terms of alloy formation and consequently, a diminished Pt ensemble size.<sup>31</sup> In both these works, the change in the dipole–dipole interactions of approximately 10 cm<sup>−1</sup> was considered to be substantial. For the present work, the monometallic Pt and the reduced fresh Pt1Cu1 had dipole–dipole shifts of 35 and 25 cm<sup>−1</sup>, respectively, and Pt1Cu3 displayed no dipole–dipole interaction whatsoever.

The fact that the CO adsorbed on Pt in the Pt1Cu3 can be removed by simple evacuation (Figure 9) at ambient temperature provides further evidence that Pt and Cu in this catalyst are atomically mixed. For monometallic Pt, adsorbed CO is stable in a vacuum at ambient temperature.<sup>32</sup> Similar to the Pt1Cu1, the band of CO adsorbed on Cu at 2135 cm<sup>−1</sup> is independent of CO surface coverage and is 40 cm<sup>−1</sup> higher than for CO linearly adsorbed on supported metallic Cu.<sup>18,24</sup> Thus, it is reasonable to conclude that the Pt and Cu in the Pt1Cu3 catalyst are alloyed.

It is also important to consider why preheating the Pt1Cu1 catalyst used in the CH<sub>2</sub>Cl–CH<sub>2</sub>Cl + H<sub>2</sub> reaction in a CO atmosphere at 473 K results in an increase in the singleton frequency for linearly adsorbed CO on Pt to 2052 cm<sup>−1</sup> (ligand effect) and the disappearance of CO dipole–dipole interactions (ensemble size effect) in comparison to the reduced fresh PtCu1 catalyst (Figure 8). The increase in the singleton frequency can be attributed to the modification of electronic properties of Pt by chemisorbed chlorine atoms formed during hydrodechlorination of CH<sub>2</sub>Cl–CH<sub>2</sub>Cl or chemisorbed oxygen resulting from CO dissociation on Pt at the temperature as high as 473 K.<sup>33,34</sup> Because of their high electronegativity, chemisorbed chlorine and oxygen atoms will increase the singleton frequency of linearly adsorbed CO by withdrawing electron density from Pt. Dissociation of CO on the used PtCu1 may cause an enrichment of the catalyst surface in Cu because of the higher binding energy of oxygen to Cu than to Pt.<sup>35–38</sup> The Cu atoms together with the carbon formed in the CO dissociation reaction may split Pt ensembles, which results in the elimination of dipole–dipole interaction between the CO molecules linearly adsorbed on Pt in the Pt1Cu1 catalyst preheated in CO at 473 K.

The idea that blocking, or limiting, the size of the Pt ensembles suppresses hydrogenation activity is borne out from the experiments when CO is added to the reaction stream. A small amount of CO in the reaction mixture increases the selectivity of the Pt1Cu3 catalyst toward ethylene, up to 100%, at the expense of ethane. The used Pt1Cu1 catalyst preheated in CO also selectively forms ethylene when CO is present in the reaction mixture. Moreover, the kinetics of hydrocarbon product accumulation shown in Figure 4 provides evidence that ethylene is a primary product of the CH<sub>2</sub>Cl–CH<sub>2</sub>Cl dehalogenation reaction. The reversible effect of CO addition on the selectivity of both Pt1Cu1 and Pt1Cu3 in the conversion of 1,2-dichloroethane suggests that there are two types of catalytic sites: one type is responsible for the formation of ethylene (Cu) and the other type of centers catalyzes hydrogenation chemistry (Pt). The sites responsible for ethylene hydrogenation are poisoned by the addition of CO into the reaction mixture. A

dual site mechanism is certainly reasonable, considering the difference in the heat of adsorption for CO on Pt and on Cu at room temperature is 27 kcal/mol (46 and 19 kcal/mol for Pt and Cu, respectively<sup>39</sup>). This difference is sufficiently great that CO remains adsorbed strongly on Pt while it is removed from Cu by simple evacuation.<sup>29</sup> Moreover, under reaction conditions CO adsorbed on Cu atoms can be substituted for CH<sub>2</sub>Cl–CH<sub>2</sub>Cl, as it was observed at room temperature (Figure 10). The blocking Pt sites with CO forces 1,2-dichloroethane to chemisorb and dissociate exclusively on Cu.<sup>40,41</sup>

The size of both Cu and Pt ensembles on the surface of the catalysts is important for high ethylene selectivity in the CH<sub>2</sub>Cl–CH<sub>2</sub>Cl + H<sub>2</sub> reaction. When the concentration of Cu on the surface of Pt–Cu particles is low, as in the case of the reduced fresh Pt1Cu1 catalyst, the Cu sites do not contribute significantly to the conversion of 1,2-dichloroethane (Figure 1). The reaction occurs mainly on Pt sites. If any reaction intermediate does form on the limited number of Cu sites, the difference in the heat of adsorption would drive the intermediate to the Pt sites, on which hydrogenation occurs. The CO in the reaction mixture substantially decreases activity by competing strongly with CH<sub>2</sub>Cl–CH<sub>2</sub>Cl for the Pt sites.

As the concentration of Cu on the surface of Pt–Cu particles increases, the copper forms larger ensembles and its role in improving ethylene selectivity becomes pronounced (Figures 2, 4, 5). The 1,2-dichloroethane cannot compete with CO for the Pt adsorption sites (Figure 10), and it is “forced” to dissociate on Cu; ethylene is thus formed on the Cu sites. If the Cu ensemble is large enough, the surface diffusion of the ethylene precursor will not result in immediate capturing it by a Pt site followed by hydrogenation to ethane, and the precursor would desorb into the gas phase as an ethylene molecule. Naturally we are assuming the H<sub>2</sub> can still dissociate on Pt when CO is present, because Cl is not accumulating on the catalyst;<sup>42</sup> the catalyst is still active. In the integral reactor, the decrease in the ethylene selectivity with time for the Pt1Cu3 without CO (Figure 2) and for the CO pretreated Pt1Cu1 in the presence of CO with conversion (Figure 4) is explained by ethylene readsorption on Pt sites followed by hydrogenation. Apparently ethylene can successfully compete with CO for Pt sites. The heat of ethylene adsorption on Pt is within 22–30 kcal mol<sup>−1</sup>,<sup>43</sup> as opposed to 46 kcal mol<sup>−1</sup> for CO adsorbed on Pt.<sup>39</sup> The fact that the ethylene selectivity for the Pt1Cu3 catalyst with CO in the reaction mixture does not depend on the 1,2-dichloroethane conversion suggests that the Pt ensembles in this catalyst are very small. It is well-known that the energy of ethylene adsorption on Pt depends on the metal ensemble size.<sup>44–46</sup> Apparently, ethylene cannot compete with CO for an adsorption site containing less than four adjacent Pt atoms, the minimal number to form di-σ-complex of ethylene<sup>42,45,46</sup> with reasonably high adsorption energy.

Thus, ensemble size effect plays a decisive role in determining ethylene selectivity of Pt–Cu/SiO<sub>2</sub> catalysts in the CH<sub>2</sub>Cl–CH<sub>2</sub>Cl + H<sub>2</sub> reaction. The ligand effect does not seem to influence strongly the catalyst performance, because changes of the Pt electronic state of opposite character accompany similar changes in selectivity. The Pt in the Pt1Cu3 catalyst is electron-rich, while the Pt after treatment of Pt1Cu1 in CO is electron-poor compared to the monometallic Pt catalyst (Figures 6, 8, 9), yet both catalysts in the presence of CO in the reaction mixture produce ethylene instead of ethane as the main product. It is particularly difficult to visualize, then, how electronic effects can be important to selectivity change.

## Conclusion

Silica-supported monometallic Pt and bimetallic Pt–Cu catalysts with a Pt-to-Cu atomic ratio of 1 (Pt1Cu1) and 0.33 (Pt1Cu3) exhibit different selectivity patterns when exposed to 1,2-dichloroethane and H<sub>2</sub> at 473 K and atmospheric pressure. The only product of the CH<sub>2</sub>Cl–CH<sub>2</sub>Cl + H<sub>2</sub> reaction catalyzed by Pt and Pt1Cu1 in a static reactor is ethane, whereas ethylene forms over the Pt1Cu3 with selectivity of 65–80% depending on the CH<sub>2</sub>Cl–CH<sub>2</sub>Cl conversion. Treatment of the Pt1Cu1 catalyst that was already used in the CH<sub>2</sub>Cl–CH<sub>2</sub>Cl + H<sub>2</sub> reaction with CO at 473 K for 0.5 h enhances the ethylene selectivity in the presence of a small amount CO in the reaction mixture. The initial ethylene selectivity of the Pt1Cu1 in this case is 100%, gradually decreasing to 30% with the CH<sub>2</sub>Cl–CH<sub>2</sub>Cl conversion. The selectivity of the Pt1Cu3 in the presence of CO is 100% independent of the conversion.

According to an IR study of CO adsorption on the ethylene unselective Pt and Pt–Cu catalysts, the electronic state of Pt in the Pt and Pt1Cu1 is similar with the singleton frequency for linearly adsorbed CO on Pt being 2040 cm<sup>−1</sup> for both catalysts. The singleton frequency of CO adsorbed on Pt of the ethylene selective Pt1Cu3 is 2030 cm<sup>−1</sup>, whereas that of the used Pt1Cu1 treated in CO (also ethylene selective) is 2055 cm<sup>−1</sup>. The coadsorption of CO and CH<sub>2</sub>Cl–CH<sub>2</sub>Cl on the Pt1Cu3 at room temperature showed that 1,2-dichloroethane can compete with CO for adsorption sites on Cu but cannot compete for the sites on Pt.

The experimental observations described in the present paper are consistent with the idea that Pt and Cu in the reduced fresh Pt1Cu1 form alloyed Pt–Cu particles significantly enriched with Pt. The Pt and Cu in the used, CO-treated Pt1Cu1 and Pt1Cu3 catalysts are also alloyed and modified electronically. However, the electronic modification of Pt and Cu does not correlate with ethylene selectivity in the CH<sub>2</sub>Cl–CH<sub>2</sub>Cl + H<sub>2</sub> reaction. Instead, ensemble effect plays a decisive role in determining ethylene selectivity of the Pt–Cu catalysts. Small ensembles of Pt with less than four contiguous atoms surrounded with Cu are suggested to be the active sites for the hydrogen-assisted 1,2-dichloroethane dechlorination toward ethylene. Copper is the site for C–Cl bond dissociation and Pt supplies dissociated H atoms to clean the Cu of adsorbed Cl atoms regenerating metallic sites.

**Acknowledgment.** Financial support from the Department of Energy—Basic Energy Sciences (DE-FG02-95ER14539) is gratefully acknowledged.

## References and Notes

- (1) Vadlamannati, L. S.; Kovalchuk, V. I.; d'Itri, J. L. *Catal. Lett.* **1999**, 58, 173.
- (2) Vadlamannati, L. S.; Luebke, D. R.; Kovalchuk, V. I.; d'Itri, J. L. *Stud. Surf. Sci. Catal.* **2000**, 130, 233.
- (3) Luebke, D. R.; Vadlamannati, L. S.; Kovalchuk, V. I.; d'Itri, J. L. *Appl. Catal. B* **2002**, 35, 211.
- (4) Ito, L. N.; Harley, D. A.; Holbrook, M. T.; Smith, D. D.; Murchison, C. B.; Cisneros, M. D. *Eur. Patent* 0 640 574 A1, 1994.
- (5) Sachtler, W. M. H. *Vide.* **1973**, 164, 67.
- (6) Sachtler, W. M. H.; van Santen, R. A. *Adv. Catal.* **1977**, 26, 69.
- (7) Peden, C. H. F.; Goodman, D. W. *J. Catal.* **1987**, 104, 347.
- (8) Dautzenberg, F. M.; Helle, J. N.; Biloen, P.; Sachtler, W. M. H. *J. Catal.* **1980**, 63, 119.
- (9) Carter, J. L.; McVicker, G. B.; Weissman, J.; Kmak, W. S.; Sinfelt, J. H. *Appl. Catal.* **1982**, 3, 327.
- (10) Anderson, J. A. *J. Catal.* **1993**, 142, 153.
- (11) Zanier-Szydlowski, N.; Moisson, B.; Blejean, F.; Didillon, B. *Proc. SPIE—Int. Soc. Opt. Eng.* **1993**, 2089, 410.
- (12) De Menorval, L.; Chaqroune, A.; Coq, B.; Figueras, F. *J. Chem. Soc., Faraday Trans.* **1997**, 93, 3715.
- (13) Chandler, B. D.; Schabel, A. B.; Rubinstein, L. I.; Pignolet, L. H. *Chem. Ind.* **1998**, 75, 607.
- (14) Crossley, A.; King, D. A. *Surf. Sci.* **1976**, 58, 379.
- (15) Crossley, A.; King, D. A. *Surf. Sci.* **1977**, 68, 528.
- (16) Crossley, A.; King, D. A. *Surf. Sci.* **1980**, 95, 131.
- (17) King, D. A. *Springer Ser. Chem. Phys.* **1980**, 15, 179.
- (18) Toolenaar, F. J. C. M.; Stoop, F.; Ponc, V. *J. Catal.* **1983**, 82, 1.
- (19) Zaikovskii, V. I.; Ryndin, Yu. A.; Koval'chuk, V. I.; Plyasova, L. M.; Kuznetsov, B. N.; Yermakov, Yu. I. *Kinet. Catal.* **1981**, 22, 340.
- (20) Deshmukh, S. S.; Borovkov, V. Yu.; Kovalchuk, V. I.; d'Itri, J. L. *J. Phys. Chem. B* **2000**, 104, 1277.
- (21) Hammaker, R. M.; Francis, S.; Eischens, R. P. *Spectrochim. Acta* **1965**, 21, 1295.
- (22) Sheppard, N.; Nguyen, T. T. *Adv. Infrared Raman Spectrosc.* **1978**, 5, 67.
- (23) De La Cruz, C.; Sheppard, N. *Spectrochim. Acta* **1994**, A50, 271.
- (24) Toolenaar, F. J. C. M.; Reinalda, D.; Ponc, V. *J. Catal.* **1980**, 64, 110.
- (25) Primet, M. *J. Catal.* **1984**, 88, 273.
- (26) Heinrichs, B.; Delhez, P.; Schoebrechts, J.-P.; Pirard, J.-P. *J. Catal.* **1997**, 172, 322.
- (27) Heinrichs, B.; Schoebrechts, J.-P.; Pirard, J.-P. *J. Catal.* **2001**, 200, 309.
- (28) Rhodes, W. D.; Lázár, K.; Kovalchuk, V. I.; d'Itri, J. L. *J. Catal.* **2002**, 211, 173.
- (29) Sokolova, N. A.; Barkova, A. P.; Furman, D. B.; Borovkov, V. Yu.; Kazansky, V. B. *Kinet. Catal.* **1995**, 36, 434.
- (30) Chandler, B. D.; Pignolet, L. H. *Catal. Today* **2001**, 65, 39.
- (31) Shpiro, E. S.; Tkachenko, O. P.; Jaeger, N. I.; Schulz-Ekloff, G.; Grunert, W. *J. Phys. Chem. B* **1998**, 102, 3798.
- (32) Ponc, V.; Bond, G. C. *Catalysis by Metal and Alloys*; Elsevier: Amsterdam, 1995.
- (33) Boudart, M. *Adv. Catal.* **1969**, 20, 153.
- (34) McCrear, K. R.; Parker, J.; Chen, P.; Somorjai, G. Abstr. Pap.—Am. Chem. Soc. 2001, 221st COLL-183.
- (35) Shustorovich, E.; Bell, A. T. *Surf. Sci.* **1992**, 268, 397.
- (36) Grimblot, J.; Luntz, A. C.; Fowler, D. E. *J. Electron Spectrosc. Relat. Phenom.* **1990**, 52, 161.
- (37) Luntz, A. C.; Grimblot, J.; Fowler, D. E. *Phys. Rev. B* **1989**, 39, 12903.
- (38) Anderson, J. R. *Structure of Metallic Catalysts*; Academic Press: London, 1975.
- (39) Somorjai, G. A. *Introduction to Surface Chemistry and Catalysis*; Wiley: New York, 1994.
- (40) Walter, W. K.; Jones, R. G.; Waugh, K. S.; Bailey, S. *Catal. Lett.* **1994**, 24, 333.
- (41) Yang, M. X.; Sarc, S.; Bent, B. E. *Langmuir* **1997**, 13, 229.
- (42) Linke, R.; Schneider, U.; Busse, H.; Becker, C.; Schroder, U.; Castro, G. R.; Wandelt, K. *Surf. Sci.* **1994**, 307, 407.
- (43) Passos, F. B.; Schmal, M.; Vannice, M. A. *J. Catal.* **1996**, 160, 118.
- (44) Windham, R. G.; Koel, B. E.; Paffett, M. T. *Langmuir* **1988**, 4, 1113.
- (45) Paffett, M. T.; Gebhard, S. C.; Windham, R. G.; Koel, B. E. *Surf. Sci.* **1989**, 223, 449.
- (46) Cortright, R. D.; Dumesic, J. A. *J. Catal.* **1994**, 148, 771.